


Hyperpolarized Metabolic and Parametric CMR Imaging of Longitudinal Metabolic-Structural Changes in Experimental Chronic Infarction

Journal Article**Author(s):**

Fuetterer, Maximilian; Traechtler, Julia; Busch, Julia; Peereboom, Sophie Marie; Dounas, Andreas; Manka, Robert; Weisskopf, Miriam; [Cesarovic, Nikola](#) ; Stoeck, Christian Torben; Kozerke, Sebastian

Publication date:

2022-11-16

Permanent link:

<https://doi.org/10.3929/ethz-b-000583905>

Rights / license:

[Creative Commons Attribution-NonCommercial-NoDerivatives 4.0 International](#)

Originally published in:

Journal of the American College of Cardiology. Cardiovascular Imaging 15(12), <https://doi.org/10.1016/j.jcmg.2022.08.017>

ORIGINAL RESEARCH

Hyperpolarized Metabolic and Parametric Cardiovascular Magnetic Resonance Imaging of Longitudinal Metabolic-Structural Changes in Experimental Chronic Infarction

Maximilian Fuetterer, PhD,^a Julia Traechtler, MSc,^a Julia Busch, PhD,^a Sophie Marie Peereboom, PhD,^a Andreas Dounas, MSc,^a Robert Manka, MD,^b Miriam Weisskopf, DVM,^c Nikola Cesarovic, DVM, PhD,^{c,d} Christian Torben Stoeck, PhD,^{a,c} Sebastian Kozerke, PhD^a

ABSTRACT

BACKGROUND Prolonged ischemia and myocardial infarction are followed by a series of dynamic processes that determine the fate of the affected myocardium toward recovery or necrosis. Metabolic adaptations are considered to play a vital role in the recovery of salvageable myocardium in the context of stunned and hibernating myocardium.

OBJECTIVES The potential of hyperpolarized pyruvate cardiac magnetic resonance (CMR) alongside functional and parametric CMR as a tool to study the complex metabolic-structural interplay in a longitudinal study of chronic myocardial infarction in an experimental pig model is investigated.

METHODS Metabolic imaging using hyperpolarized [^{13}C] pyruvate and proton-based CMR including cine, T_1/T_2 relaxometry, dynamic contrast-enhanced, and late gadolinium enhanced imaging were performed on clinical 3.0- and 1.5-T MR systems before infarction and at 6 days and 5 and 9 weeks postinfarction in a longitudinal study design. Chronic myocardial infarction in pigs was induced using catheter-based occlusion and compared with healthy controls.

RESULTS Metabolic image data revealed temporarily elevated lactate-to-bicarbonate ratios at day 6 in the infarcted relative to remote myocardium. The temporal changes of lactate-to-bicarbonate ratios were found to correlate with changes in T_2 and impaired local contractility. Assessment of pyruvate dehydrogenase flux via the hyperpolarized [^{13}C] bicarbonate signal revealed recovery of aerobic cellular respiration in the hibernating myocardium, which correlated with recovery of local radial strain.

CONCLUSIONS This study demonstrates the potential of hyperpolarized CMR to longitudinally detect metabolic changes after cardiac infarction over days to weeks. Viable myocardium in the area at risk was identified based on restored pyruvate dehydrogenase flux. (J Am Coll Cardiol Img 2022;■:■-■) © 2022 The Authors. Published by Elsevier on behalf of the American College of Cardiology Foundation. This is an open access article under the CC BY-NC-ND license (<http://creativecommons.org/licenses/by-nc-nd/4.0/>).

From the ^aInstitute for Biomedical Engineering, University and ETH Zurich, Zurich, Switzerland; ^bDepartment of Cardiology, University Heart Center, University Hospital Zurich, Zurich, Switzerland; ^cDivision of Surgical Research, University Hospital Zurich, Zurich, Switzerland; and the ^dInstitute of Translational Cardiovascular Technologies, ETH Zurich, Zurich, Switzerland. The authors attest they are in compliance with human studies committees and animal welfare regulations of the authors' institutions and Food and Drug Administration guidelines, including patient consent where appropriate. For more information, visit the [Author Center](#).

Manuscript received April 28, 2022; revised manuscript received August 10, 2022, accepted August 24, 2022.

**ABBREVIATIONS
AND ACRONYMS****AAR** = area at risk**CMR** = cardiac magnetic resonance**ECV** = extracellular volume**EF** = ejection fraction**FDG** = fluorodeoxyglucose**I/R** = ischemia/reperfusion**LDH** = lactate dehydrogenase**LGE** = late gadolinium enhanced**LV** = left ventricle**MI** = myocardial infarction**PDH** = pyruvate dehydrogenase**SNR** = signal-to-noise ratio

Cardiac magnetic resonance (CMR) has become a key diagnostic modality for the assessment of myocardial infarction (MI). Prolonged ischemia leads to MI inside myocardial tissue, which in turn incurs structural and metabolic changes in the affected territories. Because mortality and morbidity is closely associated with the extent of necrosis or fibrotic scarring post-MI, most therapeutic options focus on reperfusion and salvation of affected myocardial tissue of the area-at-risk (AAR).¹

Salvageable myocardial tissue, as opposed to necrotic regions, remains metabolically viable, despite apparent loss of contractile function. Depending on the duration and severity of ischemia, stunned and hibernating myocardium results.² In both scenarios,

metabolic adaptations are expected, and contractile impairment remains reversible.³

Prolonged ischemia before reperfusion (I/R) entails a series of dynamic healing processes with varying timescales that are accompanied by swelling and edema around the infarcted territory. In preclinical animal models, the edematous response to I/R has been shown to follow a bimodal pattern, with extracellular edema that subsides within the first 24 hours, and a deferred second “healing” phase that is accompanied by infiltration of inflammatory cells and peaks approximately 7 days post-I/R.⁴ Maintaining cell function under these conditions is directly linked to energy metabolism,⁵ which has been suggested to regulate fatty acid oxidation, activate pyruvate dehydrogenase (PDH), and thereby enhance citric acid cycle activity.⁶

Clinical, proton-based CMR allows assessment of the structural and functional state of the heart in terms of morphology, perfusion, necrosis, and scarring, using dynamic contrast-enhanced and late gadolinium enhanced (LGE) imaging, myocardial blood flow and scar volume can be quantified, whereas cine imaging allows the calculation of ventricular volumes, ejection fractions (EFs), and tissue strains. Quantitative T₁ and T₂ parameter mapping informs on the degree of intracellular and extracellular edema, hemorrhage, and development of fibrosis. Although the clinical implication of these parameters is relatively well understood and recommendations for study endpoints are available,⁷ they do not convey information on the underlying metabolic state as a potential additional target for interventions.⁸

Hyperpolarization by dissolution dynamic nuclear polarization⁹ allows one to enhance the signal of ¹³C-labelled biomolecules by orders of magnitude,

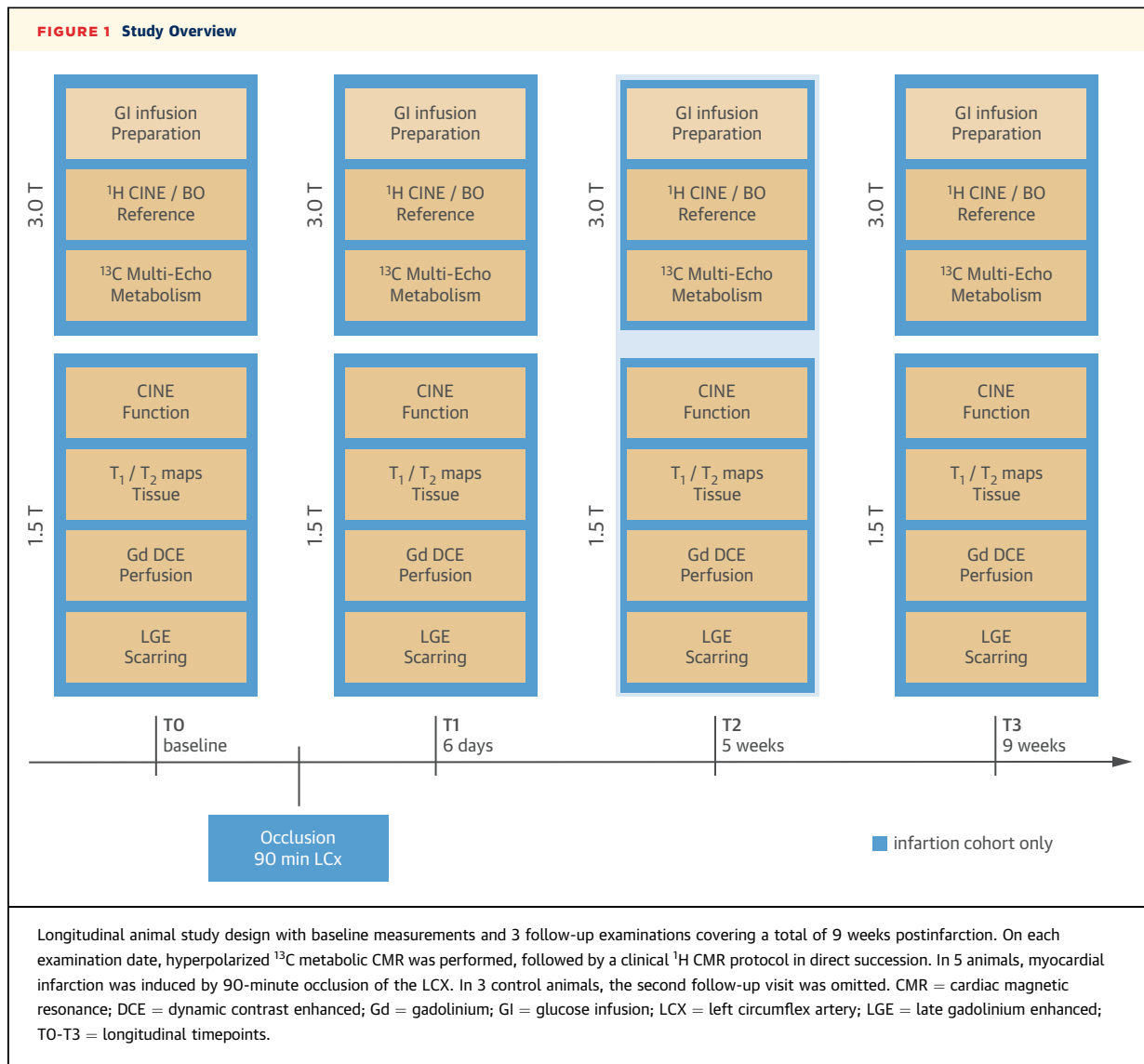
thereby addressing the intrinsic signal-to-noise ratio (SNR) limitations associated with ¹³C CMR imaging and spectroscopy. Due to its favorable physical and biological properties, [1-¹³C] pyruvate is the most widely used probe to date.¹⁰ Pyruvate is rapidly taken up into the cell and is then metabolized into [1-¹³C] lactate and [1-¹³C] alanine inside the cytosol, probing lactate dehydrogenase (LDH) and alanine transaminase activity. Simultaneously, PDH activity/tricarboxylic acid cycle flux inside the mitochondria is accessible via the [¹³C] bicarbonate readout. Several preclinical¹¹⁻¹⁴ and ongoing clinical translation trials¹⁵⁻¹⁷ have demonstrated the method’s potential of supplementing structural and functional CMR by probing these critical checkpoints in the metabolic pathway.¹⁸ Fundamentally, PDH flux is essential for cell viability, thereby identifying healthy or salvageable tissue and is up-regulated under higher energy demand.¹⁹ Increased LDH activity associates with adaptations to anaerobic conditions in the acute ischemic heart. Probing the relative contributions of PDH (aerobic) and LDH (anaerobic) in cellular respiration therefore offers a window to metabolic processes during acute infarction and subsequent recovery.

Although MI and I/R have previously been studied with hyperpolarized ¹³C CMR in rodents and porcine models, existing studies were limited to a few acute time points at which metabolism was assessed.^{11,13,20,21} The work at hand therefore constitutes the first longitudinal assessment of myocardial metabolism postinfarction in large animals on clinical magnetic resonance systems. By monitoring the metabolic states during the course of 9 weeks, in conjunction with clinical CMR protocols, the presented data ties together existing CMR endpoints with metabolic markers available with hyperpolarized ¹³C CMR.

METHODS

STUDY DESIGN. A total of 8 pigs (5 infarctions, 3 controls) were examined using a longitudinal study design as outlined in **Figure 1**. After baseline measurements (T₀), MI was induced using catheter-based 90-minute occlusion followed by reperfusion of the left circumflex artery. Hyperpolarized ¹³C and clinical ¹H CMR images were acquired at preintervention baseline (T₀), as well as 6 days (T₁), 5 weeks (T₂), and 9 weeks (T₃) postinfarction. For the control cohort, the follow-up timepoint at 5 weeks (T₂) was omitted.

All procedures and protocols were performed on regulatory approval and in accordance with strict animal protection laws. Continuous monitoring of vital parameters, as well as frequent blood gas



analysis was performed throughout the experiments. A detailed description of animal handling is provided in the [Supplemental Methods](#).

CMR IMAGING. Hyperpolarized metabolic CMR imaging was performed on a clinical multinuclei 3.0-T wide-bore scanner, whereas functional, parametric, and contrast-enhanced CMR imaging was performed consecutively on a clinical 1.5-T system (Philips).

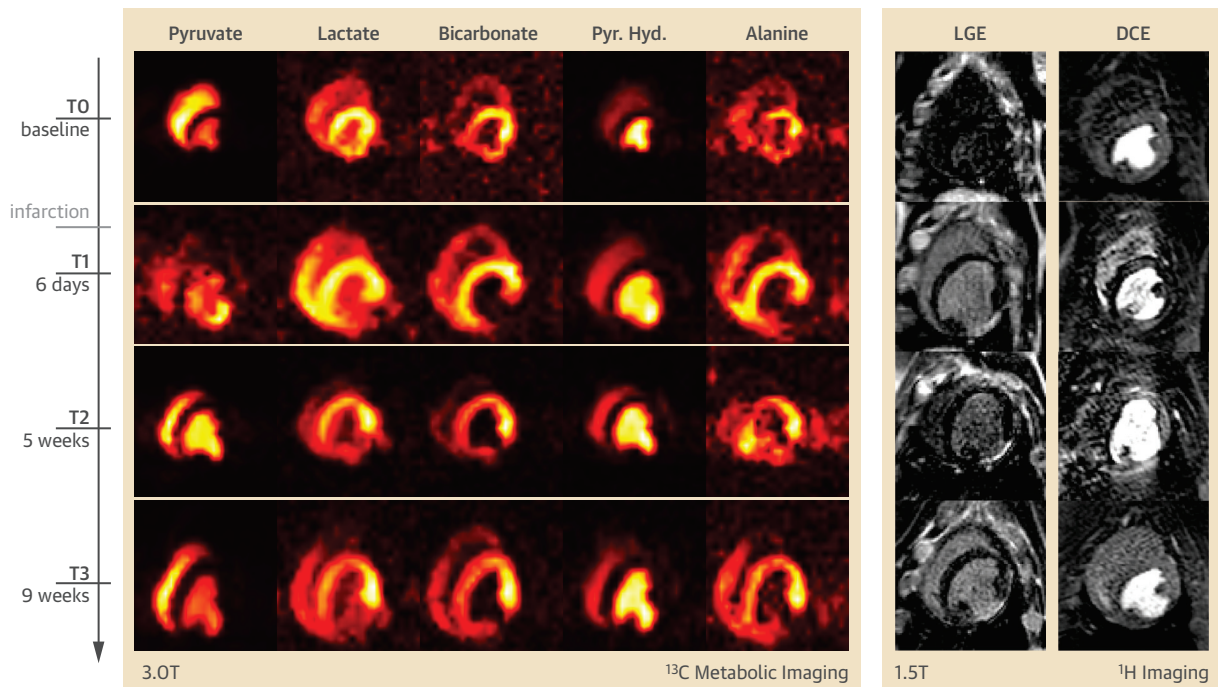
Metabolic hyperpolarized ^{13}C imaging was performed with a customized spatial-spectral excitation, multi echo-shifted single-shot echo planar imaging sequence based on an extended IDEAL approach.²² The clinical ^1H CMR imaging protocol comprised whole-heart cine imaging for functional assessments, whole-heart T_1 and T_2 mapping, dynamic contrast-enhanced perfusion, and LGE imaging. Protocol

parameters were chosen in accordance with clinical practice.

A detailed description of the preparation of the hyperpolarized injection, as well as the corresponding sequence parameters and underlying signal model is provided in the [Supplemental Methods and Supplemental Figure 1](#).

IMAGE RECONSTRUCTION AND DATA PROCESSING.

Metabolic ^{13}C images were reconstructed from CMR raw data in MRecon (GyroTools LLC) using a customized conjugate gradient descent algorithm.²³ The resulting metabolite images for pyruvate, pyruvate hydrate, alanine, lactate, and bicarbonate were zero-filled to $1 \times 1 \text{ mm}^2$ in-plane resolution and manually segmented using overlays of ^{13}C and anatomical ^1H reference images. Dynamic signal

FIGURE 2 Longitudinal Image Series of ^{13}C Metabolic CMR

Exemplary longitudinal image set of 1 animal (infarction #2) over the course of 4 measurements, covering 9 weeks postinfarction. Acute infarction in the inferior lateral wall is well depicted on downstream ^{13}C metabolite images, with metabolic activity in the border zone returning at later timepoints (left). Infarct location and extent is confirmed by contrast-enhanced ^1H CMR (right). Abbreviations as in Figure 1.

intensity curves were extracted and baseline-corrected from 4 myocardial sectors aligned such that the AAR including the infarction area was contained in 1 sector, whereas the other 3 sectors covered healthy remote myocardium. The corresponding area under the curve (AUC) values were calculated for each metabolite and sector and normalized with the AUC of the arterial input function as a surrogate for first order kinetic rate constants (Met2Pyr).²⁴ The arterial input function signals were obtained from signal intensities in the left ventricle (LV) in the flip-angle corrected pyruvate input image. Ratios of lactate to bicarbonate AUCs (Lac2Bic), as well as relative contributions of each metabolite (lactate, bicarbonate, alanine) to the total downstream ^{13}C signal (Met2TC) were calculated for each sector.

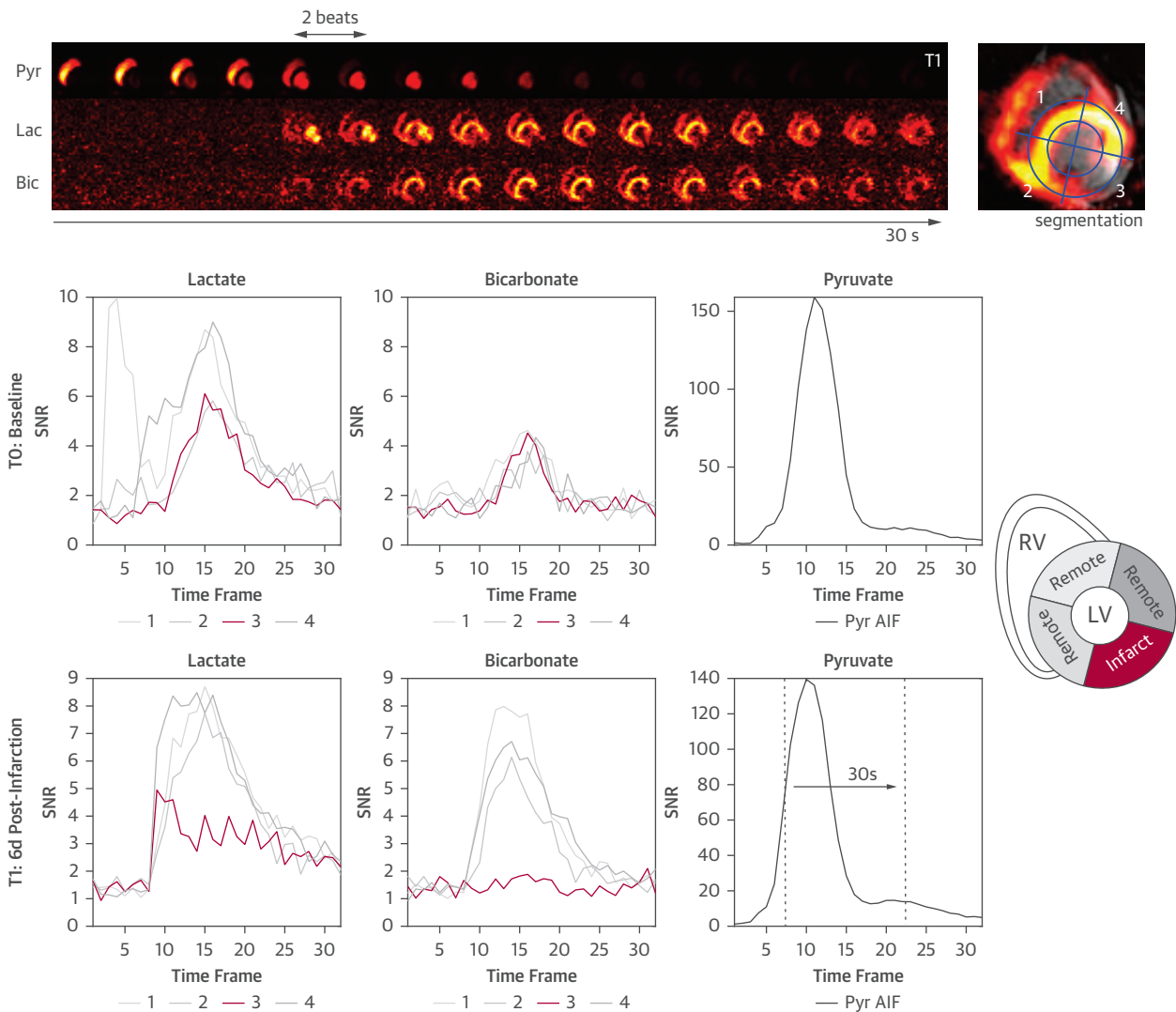
Proton CMR images were segmented and analyzed in GTVolume (GyroTools LLC) to determine ventricular volume and mass, as well as left-ventricular EF. Infarction and remote sites were manually segmented on LGE images to calculate infarction extracellular volume (ECV) and native/enhanced T_1 and T_2 values for both areas. Localized radial strain values were

derived from cine images in the infarcted inferior lateral sector, as well as the septal region for peak systole and diastole.

RESULTS

Unless otherwise stated, values are reported as mean \pm SD. Physiological parameters of the study cohort are summarized in the [Supplemental Results and Supplemental Table 1](#).

HYPERPOLARIZED ^{13}C METABOLIC IMAGING. Dynamic image series acquired after injection of hyperpolarized $[1-^{13}\text{C}]$ pyruvate were of high spatial, spectral, and temporal fidelity reflective of the current state-of-the-art,^{10,25} revealing conversion of $[1-^{13}\text{C}]$ pyruvate into its downstream metabolites $[1-^{13}\text{C}]$ lactate, $[^{13}\text{C}]$ bicarbonate, and $[1-^{13}\text{C}]$ alanine. An exemplary longitudinal image series along with contrast-enhanced ^1H CMR images is presented in [Figure 2](#). Corresponding dynamic signal intensities in the 3 remote and 1 infarction sectors are presented in [Figure 3](#). Reduced signal caused by impaired perfusion 6 days postinfarction (T1) is apparent in the

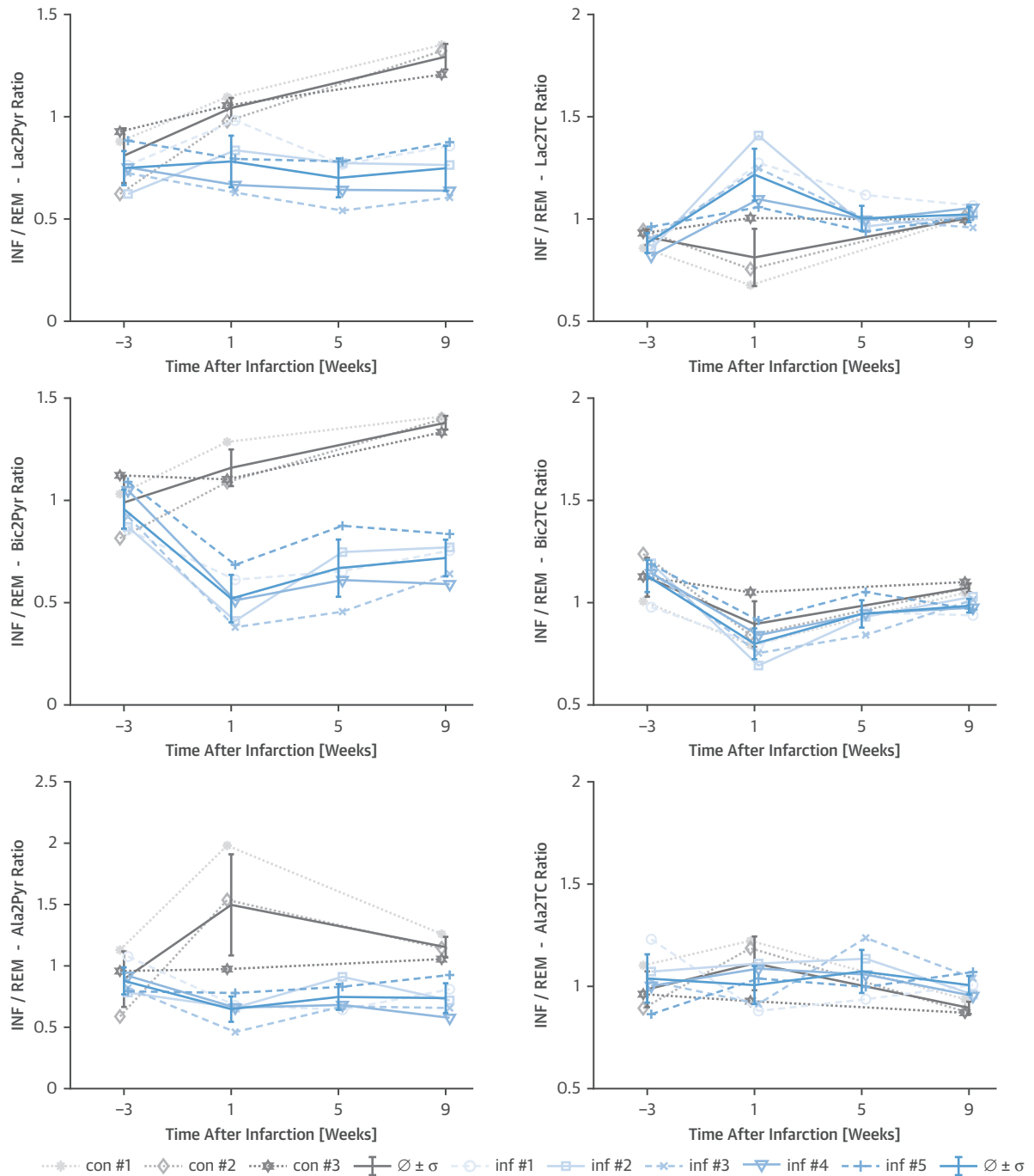
FIGURE 3 Exemplary Dynamic Metabolite Data Obtained Using Hyperpolarized ^{13}C CMR

(Top) Dynamic image series of injected [$1\text{-}^{13}\text{C}$] pyruvate bolus and downstream metabolites [$1\text{-}^{13}\text{C}$] lactate, [^{13}C] bicarbonate probing glycolysis in real-time (animal infarction #2). **(Bottom)** Metabolite signal curves derived from a 4-sector segmentation at baseline (T0) and 1 week postinfarction (T1), normalized to reflect SNR. Whereas anaerobic conversions into lactate via LDH is still observable in the AAR (sector 3, red), decarboxylation into acetyl-CoA is diminished as illustrated by the lack of [^{13}C] bicarbonate signal. AAR = area at risk; AIF = arterial input function; Bic = bicarbonate; Lac = lactate; LDH = lactate dehydrogenase; LV = left ventricle; Pyr = pyruvate; RV = right ventricle; SNR = signal-to-noise ratio.

infarcted sector, with residual signal originating from the salvageable myocardium. Metabolite signals in the myocardium appear with a delay of approximately 5 heartbeats after the LV pyruvate input.

To account for individual variations in metabolism between animals, metabolic markers are presented in **Figure 4** in a per-animal fashion as ratios between infarction and remote area, thereby providing an intra-animal reference for metabolic base activity at time of imaging (Normalized

metabolite AUC ratios for both areas separately are presented in the Supplemental Results, i.e. **Supplemental Figure 2 and Supplemental Table 2**). At baseline, relative lactate, bicarbonate, and alanine signals were found to be comparable between control and infarction groups. After intervention, metabolic conversion of pyruvate remained inhibited in the scarred infarction area as a result of reduced substrate availability and lack of functional tissue. Relative contributions of lactate and

FIGURE 4 Ratios of Metabolic Markers Between Infarction and Remote Area per Animal

Downstream metabolite ratios expressed as ratios of AUC values derived from mean signals in infarction/remote sectors (inf/rem) of the myocardium, normalized by pyruvate input AUC (Met2Pyr) (**left column**) or normalized by total carbon (lactate + bicarbonate + alanine) (Met2TC). For the infarction cohort, infarcted sectors including the AAR show reduced overall metabolic activity compared with the remote area, with relative increase of lactate and decrease of bicarbonate 1 week postinfarction, indicative of increased anaerobic glycolysis. Mean (∅) ± SD (σ) over the infarction (inf) and control (con) cohorts. AUC = area under the curve; Ala2Pyr = alanine to pyruvate ratio; Ala2TC = alanine to total carbon ratio; Bic2Pyr = bicarbonate to pyruvate ratio; Bic2TC = bicarbonate to total carbon ratio; INF = infarcted myocardium; Lac2Pyr = lactate to pyruvate ratio; Lac2TC = lactate to total carbon ratio; REM = remote myocardium; other abbreviations as in [Figure 3](#).

bicarbonate to the total carbon signal (Lac2TC/Bic2TC) indicate a temporary inhibition of PDH with a simultaneous enhanced LDH activity at 6 days postinfarction.

¹H IMAGING. Functional and volumetric CMR parameters derived from cine and LGE imaging are summarized in [Table 1](#). In accordance with animal growth, LV mass and end-diastolic volume developed to a similar common endpoint for the infarction and control cohorts, despite larger organ size at baseline in the control group. Average infarction mass was found to be 7.4 ± 3.6 g with an average 54% increase during 9 weeks postinfarction. Scar transmural was found to be >80% in all cases. Stroke volume and EF analysis revealed a persistent reduction after intervention in comparison with the control group, as well as increased end-systolic LV volumes.

Parameter mapping results for native/enhanced T₁, T₂, and ECV are summarized in [Table 2](#).

IDENTIFYING HIBERNATING MYOCARDIUM. Metabolic viability, reflected by PDH activity in terms of detectable [¹³C] bicarbonate signal, is shown in [Figure 5](#) for all animals of the infarction cohort. In the acute stage, the infarcted territory is clearly depicted as signal void in the [¹³C] bicarbonate signal. During the course of the study, the circumferential extent of metabolically inactive myocardium is noticeably reduced, indicating recovery of aerobic glycolysis in the hibernating/salvageable myocardium.

[Figure 6](#) illustrates that the complementary multimodal markers reveal the different types of myocardial tissue damage in the context of MI. Acute injury at 6 days postinfarction is characterized by increased high-sensitivity Troponin T levels, increased relative anaerobic metabolic activity (Lac2Bic) in the infarcted territory, elevated T₂ values associated with extracellular edema,²⁶ and ECV augmentation associated with necrosis. Simultaneously, contractile function (local radial strain) is reduced in the infarcted territory, linking functional impairment to metabolic activity. In both ¹³C and ¹H CMR, the initial effects are transient, as the values at 5 weeks postinfarction approach those of the control group. Although signs of acute edema and metabolic adaptations in the AAR subside fully over the course of the study, local contractile function remains partly impaired, and persistent fibrosis is revealed by elevated ECV and native T₁ values.

[Figure 7](#) illustrates the relationship between degree of myocardial edema (T₂ values)/local radial strain and increased LDH (Lac2Bic) in the infarct zone over time. Data obtained 6 days postinfarction form a cluster that differs from baseline measurements, as

TABLE 1 Functional and Volumetric Parameters Derived From ¹H CMR

	T0 (Baseline)	T1 (6 d)	T2 (5 wk)	T3 (9 wk)
LV mass, g				
Infarction	43 ± 3	51 ± 10	62 ± 13	77 ± 14
Control	52 ± 10	61 ± 7	-	89 ± 6
Infarction mass, g				
Infarction	NA	5.7 ± 2.8	7.6 ± 3.3	8.8 ± 4.5
Control	NA	NA	NA	NA
LV volume systolic, mL				
Infarction	43 ± 4	57 ± 10	69 ± 7	81 ± 8
Control	47 ± 9	51 ± 9	-	70 ± 3
LV volume diastolic, mL				
Infarction	85 ± 7	108 ± 14	122 ± 16	152 ± 18
Control	98 ± 18	103 ± 16	-	150 ± 7
Stroke volume, mL				
Infarction	42 ± 6	51 ± 5	53 ± 15	71 ± 11
Control	51 ± 10	56 ± 6	-	80 ± 5
LV ejection fraction, %				
Infarction	50.5 ± 4.4	47.3 ± 3.3	42.6 ± 8.0	46.8 ± 2.7
Control	52.3 ± 2.2	54.2 ± 3.1	-	53.3 ± 0.9
Radial strain inf-lat, %				
Infarction	49.2 ± 8.7	24.6 ± 10.5	37.1 ± 11.4	35.8 ± 11.4
Control	50.5 ± 11.0	49.8 ± 1.3	-	54.3 ± 5.2

CMR = cardiac magnetic resonance; inf-lat = inferiorlateral segment; LV = left ventricular; - = not applicable.

well as relative to data at 5 weeks and 9 weeks postinfarction. In 1 animal (infarction #3), T₂ values remained increased throughout the chronic stage with sustained contractile impairment, whereas the metabolic state normalized similarly to other animals.

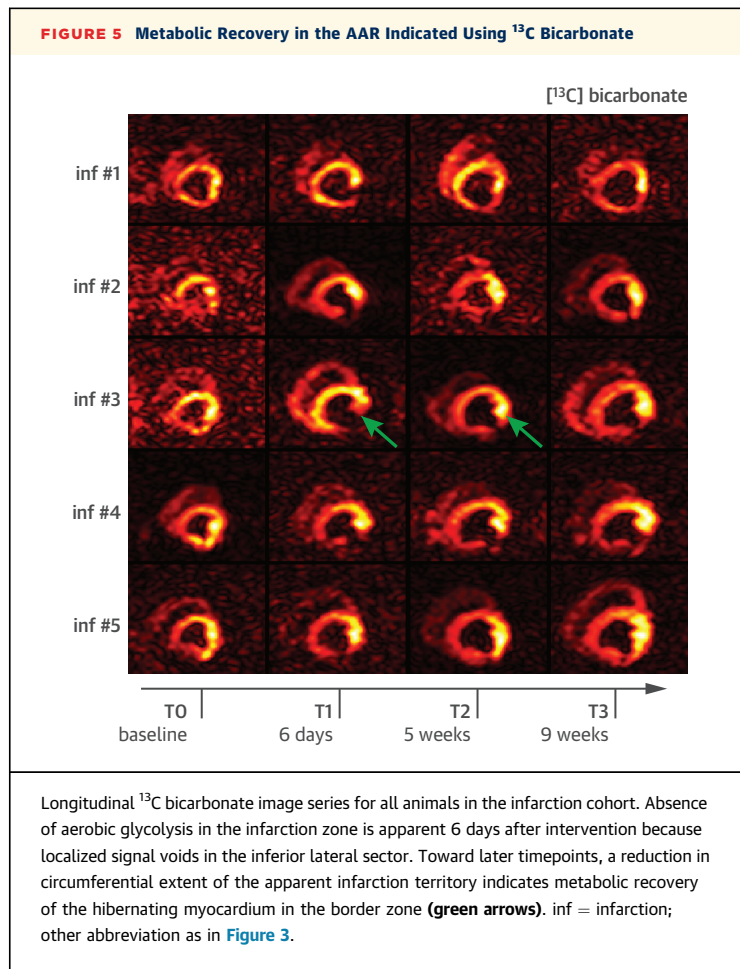
DISCUSSION

In this work, we have demonstrated the feasibility of detecting metabolic and structural longitudinal changes after cardiac infarction using hyperpolarized

TABLE 2 Parameter Mapping Results Derived From ¹H CMR in the Infarction Zone

	T0 (Baseline)	T1 (6 d)	T2 (5 wk)	T3 (9 wk)
T1 native, ms				
Infarction	970 ± 24	1,080 ± 74	1,135 ± 29	1,106 ± 83
Control	975 ± 7	964 ± 35	NA	894 ± 42
T1 enhanced, ms				
Infarction	684 ± 36	515 ± 35	379 ± 117	383 ± 102
Control	578 ± 65	549 ± 37	NA	506 ± 23
T2, ms				
Infarction	53 ± 8	81 ± 2	64 ± 11	69 ± 12
Control	56 ± 5	58 ± 3	NA	56 ± 9
ECV, %				
Infarction	34 ± 3	76 ± 4	87 ± 7	83 ± 8
Control	34 ± 4	34 ± 2	NA	30 ± 3

ECV = extracellular volume; other abbreviations as in [Table 1](#).



and conventional CMR. Elevated lactate-to-bicarbonate ratios were detected at day 6 after infarction as an indicator of increased anaerobic cellular respiration as well as monocyte/macrophage activity as part of the healing response. Metabolic changes were in synch with temporarily increased T_2 values associated with edematous swelling, as well as reversible impaired local contractility. Recovery of hibernating myocardium in the AAR was identified based on restored PDH flux. The results offer further insights into the dynamic nature of myocardial adaptations on infarction.

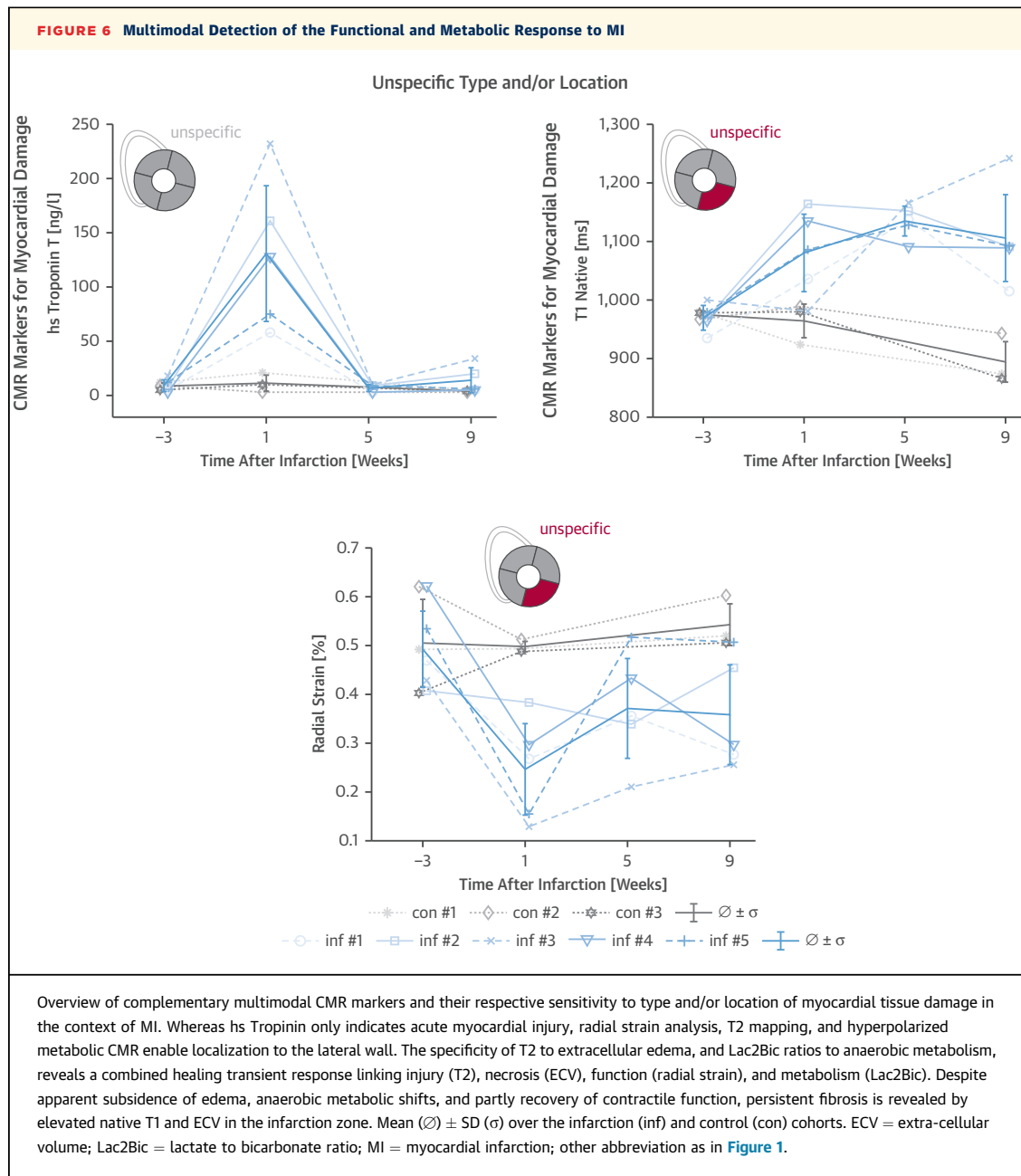
The bimodal nature of myocardial edema post-I/R injury has been established in large animal (pig) models.^{26,27} During the deferred healing wave, which peaks around 1 week after infarction and which is associated with inflammatory cell infiltration, T_2 values in the infarction territory were elevated due to increased water content of tissue.²⁸ Increased lactate-

to-bicarbonate ratios in the affected myocardium meanwhile indicate increased relative LDH activity. Although LDH is known as a key factor in anaerobic cellular respiration under ischemic conditions, increased $[1-^{13}\text{C}]$ lactate production has also been associated with the monocyte/macrophage inflammatory response.¹³ Noticeably, the observed metabolic changes follow the same transient pattern as the edema and as assessed by T_2 mapping and high-sensitivity Troponin values as markers of acute myocardial injury. Starting at 5 weeks postinfarction, edema (T_2) and metabolic responses (^{13}C) approached the data in control animals, whereas levelling off T_1 and ECV values indicate persistent fibrosis in the tissue. T_2 values remained mildly elevated compared with baseline, however, less so than seen in a study of reperfused MI in Yucatan pigs after 60 days,²⁹ indicating a different degree of persistent edema in both models.

Probing localized PDH flux via $[^{13}\text{C}]$ bicarbonate has been demonstrated to be useful in the detection of viable myocardium in the AAR, in accordance with previous work demonstrating temporary absence of PDH flux in a model of stunned myocardium by 60-minute occlusion of the left anterior descending artery.¹⁹ Despite a similar intervention, the acute metabolic response to the 90-minute occlusion of the left circumflex artery consistently induced MI, with acute metabolic responses apparent 6 days postinfarction. The additional longitudinal timepoints revealed a link between metabolic and functional recovery in the AAR on a longer timescale, more consistent with the definition of hibernating rather than stunned myocardium and a prolonged hypoperfusion and delayed neovascularization at a timescale of weeks.

Together, these findings support the previously suggested capability of hyperpolarized $[1-^{13}\text{C}]$ pyruvate to probe both inflammatory response to I/R injury, as well as transient metabolic reprogramming in the AAR toward increased anaerobic glycolysis under oxygen deprivation.

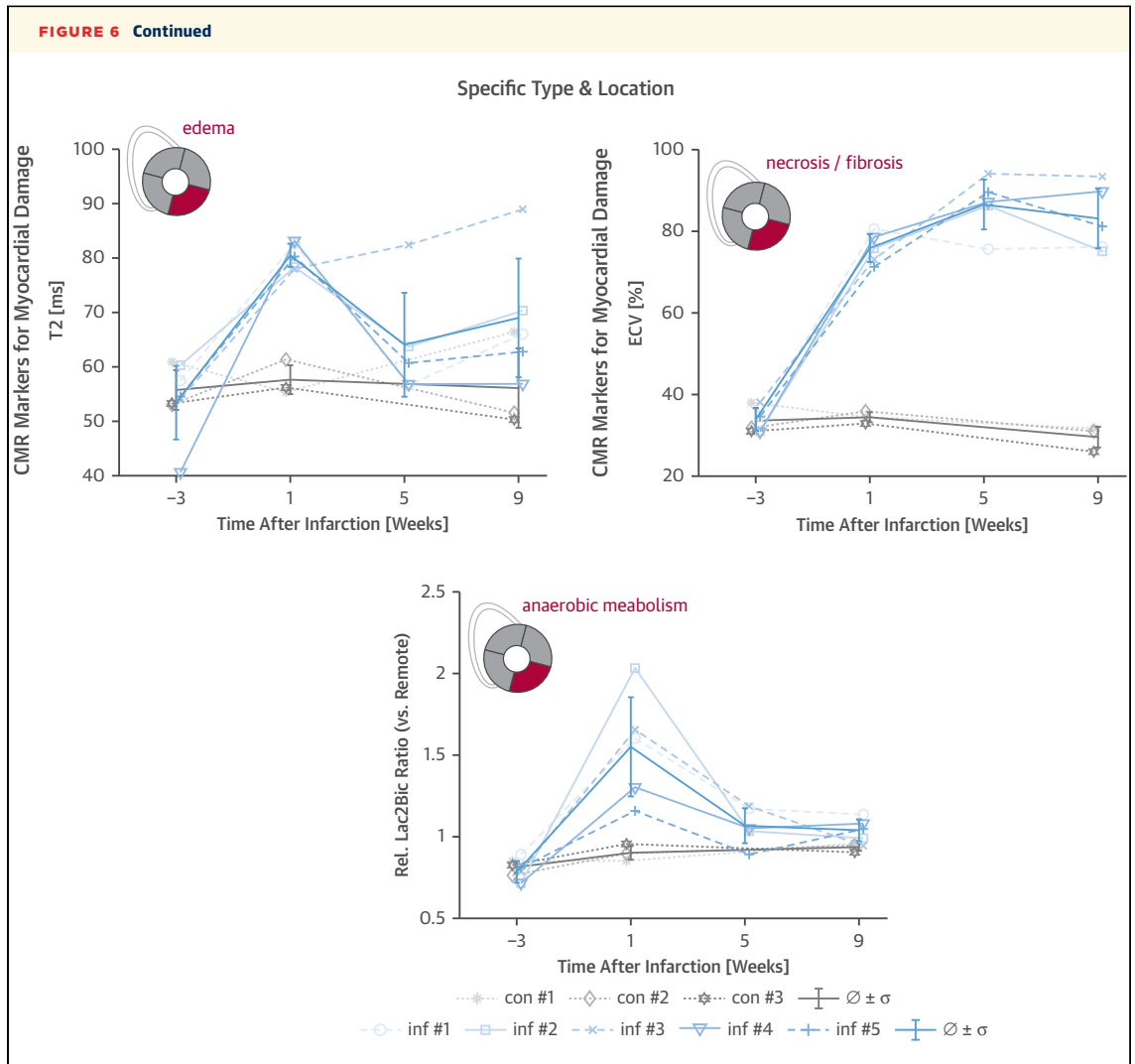
Noninvasive identification of viable myocardium with radio nuclear tracers using single-photon emission computed tomography or positron emission tomography with ^{18}F -labelled fluorodeoxyglucose (FDG) are established alternative methods for metabolic imaging of the heart. Nonetheless, their clinical use is still debated, mainly due to variable specificity and lack of benefits over classical CMR.³⁰ In contrast to hyperpolarized ^{13}C , ^{18}F -FDG undergoes only a



Continued on the next page

single conversion into ^{18}F -FDG-6-P and hence reflects primarily glucose uptake, rather than probing the glycolytic pathways inside myocytes. The ability of differentiating healthy myocardium (intact PDH flux) from oxygen-deprived tissue under stress (increased LDH flux) before necrosis makes hyperpolarized CMR a promising alternative to radio nuclear methods. The clinical value of the additional information, however, remains to be explored.

Hyperpolarized ^{13}C CMR has been used in a variety of pig models in the context of heart failure, including right ventricular heart failure,¹⁴ dilated cardiac myopathy,¹² and I/R injury.^{13,19} Although metabolic adaptations were revealed in all studies, disease-specific metabolic signatures are not immediately apparent. In absence of established reference values for healthy PDH/LDH activity, a relative increase in relative lactate-to-bicarbonate appears to be a



common marker in heart disease, albeit with different dynamics over disease progression. The presented local temporary increase in relative LDH activity at 6 days after MI is in agreement with previous studies,^{13,19} although the effects were persistent and unlocalized in right ventricular heart failure.¹⁴ This underlines the importance of multimodal CMR approaches, as well as the need for further longitudinal trials to establish optimal examination timepoints.

Comparing ratios of downstream metabolites directly (bicarbonate/lactate) normalizes for bolus variations, as well as localized and global perfusion deficits. Although not directly reflective of kinetic rate constants, this marker provides the relevant information when inhibition or up-regulation of PDH/LDH activity is suspected. Because intersubject variability in hyperpolarized ratio metric readouts is

generally large, sensitivity to adaptive processes is limited.^{19,31} In the present work, ratios between infarcted and remote myocardial signals were, therefore, used to effectively normalize for the metabolic baseline of each animal at the time of measurement (Supplemental Figure 3), as elaborated in detail in the Supplemental Discussion. Alternatively, pharmacologically induced stress and rest imaging in analogy to perfusion CMR is a promising approach to assess metabolic reserve (ie, the capability of the heart to up-regulate glycolysis under increased load).¹⁷

One major challenge when using metabolically active substrates in the context of ischemia and MI, is the high sensitivity to perfusion deficits. Affected regions suffer from impaired or absent delivery of the imaging substrate, and, as such, metabolic readouts are limited to sufficiently perfused regions. Existing

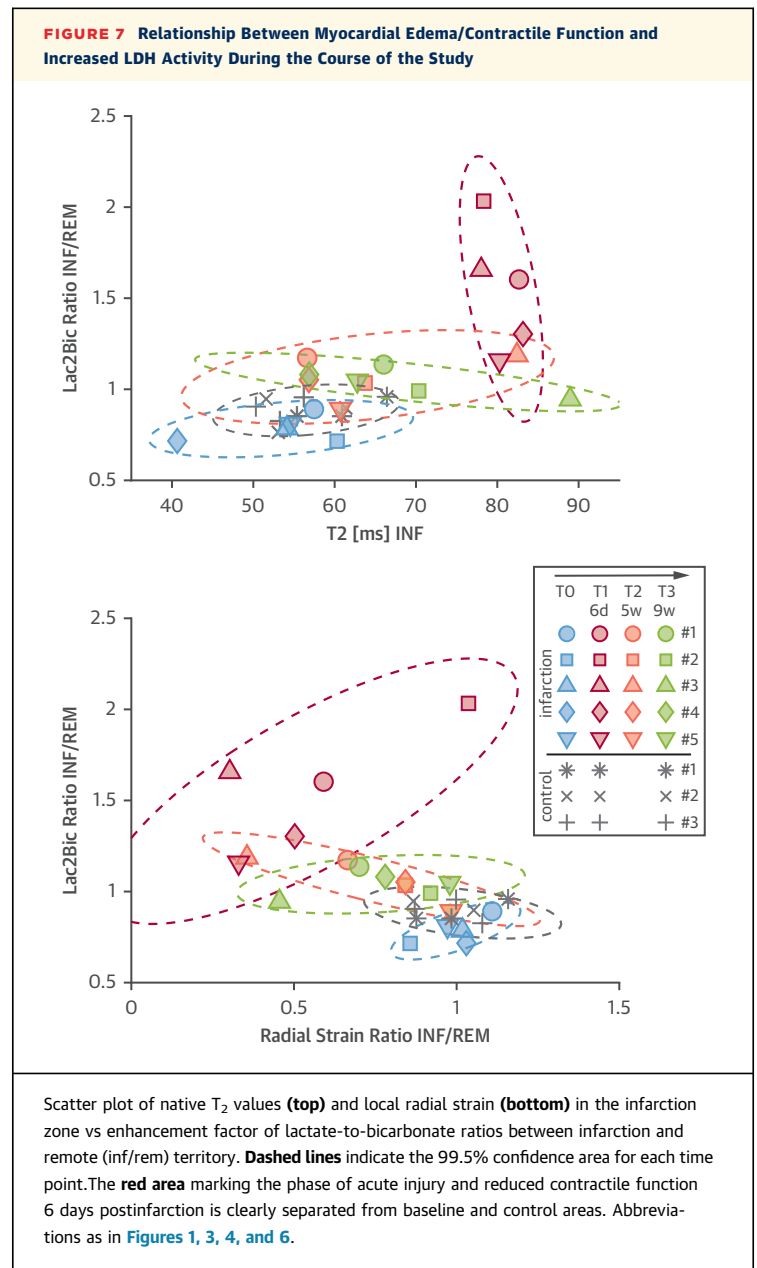
methods to acquire perfusion with hyperpolarized injections require copolarization with metabolically inert substrates such as ^{13}C urea³² or a dual-bolus approach with tailored acquisition strategies.³³ Although gadolinium-based perfusion CMR can qualitatively augment the metabolic information, the different bolus shapes, pharmacokinetics, and limited resolution of $[1-^{13}\text{C}]$ pyruvate present challenges for quantitative modelling. Given the potential value of reliable perfusion information alongside metabolic readouts, further development in this direction is, however, considered highly relevant.

At achievable resolutions and slice thicknesses for hyperpolarized CMR, analyzing PDH/LDH flux individually on a global or voxel-wise basis, therefore, likely introduces bias toward perfusion effects, rather than metabolic adaptations, and increases noise levels in the data. In this work, segmentation was hence deliberately performed on large segments to retain SNR, especially in the infarction sector where only the small border zone contributes to metabolic signal.

STUDY LIMITATIONS. Due to the ethical burdens posed by the study design, only a relatively small number of animals could be enrolled in both the intervention and control groups, which is a common limitation in interventional longitudinal CMR studies, especially given the number of examinations and total study duration for each animal. Although statistical power is not sufficient for quantitative analysis, the data obtained from the infarcted animals follows a remarkably similar trend when presented on a per-animal basis. Only 1 animal (infarction #3) deviated from the general trend with respect to native T_1 and T_2 values at later time points, which is not reflected in the metabolic markers. This particular animal exhibited the largest infarct size with pronounced subsequent signs of remodeling.

As an emerging modality, hyperpolarized CMR is still subject to ongoing methodologic improvements. Although the image quality and acquisition resolution presented herein ($5 \times 5 \times 20 \text{ mm}^3$) is considered cutting edge, such voxel sizes still inherently compromise the delineation of small regions such as the AAR. Coregistration with higher-resolution ^1H images, which could aid in the segmentation of myocardial subregions, is challenged by the limited anatomical features available in ^{13}C data. Therefore, and to improve SNR, a sector-based segmentation appears more suitable for analysis, at the risk that sectorial signals contain some amount of healthy myocardial tissue.

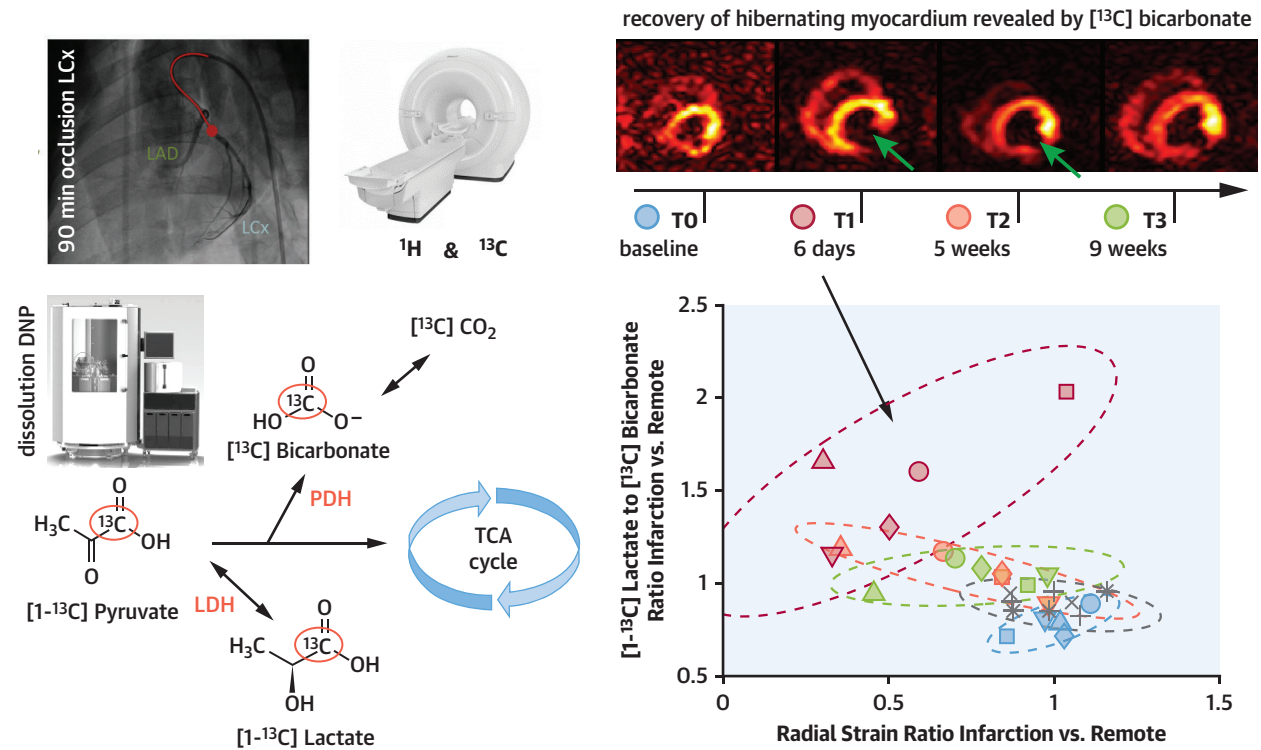
The longitudinal study design, in conjunction with bore sizes of clinical magnetic resonance systems,



required the use of juvenile animals. Although there is no particular reason to assume metabolic differences in adult swine, underlying systematic offsets cannot be ruled out.

CONCLUSIONS

This study has demonstrated the feasibility of detecting metabolic and structural longitudinal changes after cardiac infarction using hyperpolarized CMR alongside conventional CMR. Viable myocardium in the border zone of the AAR was identified

CENTRAL ILLUSTRATION Monitoring the Dynamic Response to Myocardial Infarction With Functional, Parametric, and Hyperpolarized Metabolic CMR

Fuetterer M, et al. *J Am Coll Cardiol Img.* 2022; ■(■):■-■.

Metabolic alongside functional and parametric CMR after the dynamic response to myocardial infarction in an experimental pig model in a longitudinal study design over 9 weeks. Metabolic imaging using hyperpolarized $[1-^{13}\text{C}]$ pyruvate reveals relative adaptations in the glycolytic pathway and identifies recovering viable myocardium in the border zone based on restored citric acid cycle uptake. Temporary metabolic shifts toward anaerobic glycolysis coincide with impaired contractile function and increased T_2 values. CMR = cardiac magnetic resonance.

based on restored PDH flux. Elevated lactate-to-bicarbonate ratios 1 week after infarction were detected indicative of metabolic adaptations to the hypoxic environment. The transient metabolic shifts after infarction were in synch with increased T_2 values associated with edematous swelling and locally impaired contractile function. The combination of hyperpolarized metabolic and functional CMR is hence considered a promising tool to provide further insights into the complex metabolic-structural temporal changes after cardiac infarction.

ACKNOWLEDGMENTS The authors would like to thank Constantin von Deuster for help with experimental preparations and scanning of animals, Conny Waschki for segmentation of ^1H CMR data, as well

as Thea Fleischmann and Marko Canic for animal handling and aftercare.

FUNDING SUPPORT AND AUTHOR DISCLOSURES

This research was funded in parts by the Swiss National Science Foundation, grants SNF 320030_153014, CR2313_166485, and PZ00P2 174144, as well as the Maexi Foundation, Switzerland. The authors have reported that they have no relationships relevant to the contents of this paper to disclose.

ADDRESS FOR CORRESPONDENCE: Dr Sebastian Kozerke, Institute for Biomedical Engineering, University and ETH Zurich, Gloriastrasse 35, 8092 Zurich, Switzerland. E-mail: kozerke@biomed.ee.ethz.ch. Twitter: @CMR_Zurich.

PERSPECTIVES

COMPETENCY IN MEDICAL KNOWLEDGE: The bimodal response of the heart to prolonged ischemia comprises a series of structural, functional, and metabolic processes. Hyperpolarized metabolic CMR has been shown to be able to link functional impairment to underlying metabolic adaptations during the acute healing phase. As a biomarker of cellular respiration, [¹³C] bicarbonate is able to identify viable myocardium.

TRANSLATIONAL OUTLOOK: Hyperpolarized metabolic imaging of the heart has successfully made the transition into ongoing clinical trials, including patient

cohorts with chronic MI. In addition to [¹³C] pyruvate, novel substrates that target alternative metabolic pathways are being investigated. Although the required instrumentation, pharmaceutical preparation, and, therefore, resulting cost prohibit clinical adoption of hyperpolarized imaging in its current state, ongoing efforts to simplify the overall process should greatly improve accessibility. As such, there is promise to perform hyperpolarized metabolic imaging routinely as part of clinical CMR protocols with only a few additional minutes of scan time per patient.

REFERENCES

- Ibáñez B, Heusch G, Ovize M, Van De Werf F. Evolving therapies for myocardial ischemia/reperfusion injury. *J Am Coll Cardiol*. 2015;65:1454-1471. <https://doi.org/10.1016/j.jacc.2015.02.032>
- Richard Conti C. The stunned and hibernating myocardium: a brief review. *Clin Cardiol*. 1991;14:708-712. <https://doi.org/10.1002/clc.4960140903>
- Kloner RA. Stunned and hibernating myocardium: where are we nearly 4 decades later? *J Am Heart Assoc*. 2020;9:1-11. <https://doi.org/10.1161/JAHA.119.015502>
- Fernández-Jiménez R, García-Prieto J, Sánchez-González J, et al. Pathophysiology underlying the bimodal edema phenomenon after myocardial ischemia/reperfusion. *J Am Coll Cardiol*. 2015;66:816-828. <https://doi.org/10.1016/j.jacc.2015.06.023>
- García-Dorado D, Andres-Villarreal M, Ruiz-Meana M, Insete J, Barba I. Myocardial edema: a translational view. *J Mol Cell Cardiol*. 2012;52:931-939. <https://doi.org/10.1016/j.yjmcc.2012.01.010>
- Halestrap AP. The regulation of the oxidation of fatty acids and other substrates in rat heart mitochondria by changes in the matrix volume induced by osmotic strength, valinomycin and Ca²⁺. *Biochem J*. 1987;244:159-164. <https://doi.org/10.1042/bj2440159>
- Kramer CM, Barkhausen J, Bucciarelli-Ducci C, Flamm SD, Kim RJ, Nagel E. Standardized cardiovascular magnetic resonance imaging (CMR) protocols: 2020 update. *J Cardiovasc Magn Reson*. 2020;22:1-10. <https://doi.org/10.1186/s12968-020-00607-1>
- Taegtmeyer H. Cardiac metabolism as a target for the treatment of heart failure. *Circulation*. 2004;110:894-896. <https://doi.org/10.1161/01.CIR.0000139340.88769.D5>
- Ardenkjaer-Larsen JH, Fridlund B, Gram A, et al. Increase in signal-to-noise ratio of > 10,000 times in liquid-state NMR. *Proc Natl Acad Sci U S A*. 2003;100:10158-10163.
- Wang ZJ, Ohliger MA, Larson PEZ, et al. Hyperpolarized ¹³C MRI: state of the art and future directions. *Radiology*. 2019;291:273-284. <https://doi.org/10.1148/radiol.2019182391>
- O h-Ici D, Wespi P, Busch J, et al. Hyperpolarized metabolic MR imaging of acute myocardial changes and recovery after ischemia-reperfusion in a small-animal model. *Radiology*. 2016;278:742-751. <https://doi.org/10.1148/radiol.2015151332>
- Schroeder MA, Lau AZ, Chen AP, et al. Hyperpolarized ¹³C magnetic resonance reveals early- and late-onset changes to in vivo pyruvate metabolism in the failing heart. *Eur J Heart Fail*. 2013;15:130-140. <https://doi.org/10.1093/eurjhf/hfs192>
- Lewis AJM, Miller JJ, Lau AZ, et al. Noninvasive immunometabolic cardiac inflammation imaging using hyperpolarized magnetic resonance. *Circ Res*. 2018;122:1084-10893. <https://doi.org/10.1161/CIRCRESAHA.117.312535>
- Agger P, Hyldebrandt JA, Hansen ESS, et al. Magnetic resonance hyperpolarization imaging detects early myocardial dysfunction in a porcine model of right ventricular heart failure. *Eur Heart J Cardiovasc Imaging*. 2020;21:93-101. <https://doi.org/10.1093/ehjci/jez074>
- Cunningham CH, Lau JYC, Chen AP, et al. Hyperpolarized ¹³C metabolic MRI of the human heart: initial experience. *Circ Res*. 2016;119:1177-1182. <https://doi.org/10.1161/CIRCRESAHA.116.309769>
- Rider OJ, Apps A, Miller JJJJ, et al. Noninvasive in vivo assessment of cardiac metabolism in the healthy and diabetic human heart using hyperpolarized ¹³C MRI. *Circ Res*. 2020;126(6):725-736. <https://doi.org/10.1161/CIRCRESAHA.119.316260>
- Joergensen SH, Hansen ESS, Bøgh N, et al. Detection of increased pyruvate dehydrogenase flux in the human heart during adenosine stress test using hyperpolarized [¹³C]pyruvate cardiovascular magnetic resonance imaging. *J Cardiovasc Magn Reson*. 2022;24:1-9. <https://doi.org/10.1186/s12968-022-00860-6>
- Rider OJ, Tyler DJ. Clinical implications of cardiac hyperpolarized magnetic resonance imaging. *J Cardiovasc Magn Reson*. 2013;15:93. <https://doi.org/10.1186/1532-429X-15-93>
- Lau AZ, Chen AP, Barry J, et al. Reproducibility study for free-breathing measurements of pyruvate metabolism using hyperpolarized ¹³C in the heart. *Magn Reson Med*. 2013;69:1063-1071. <https://doi.org/10.1002/mrm.24342>
- Aquaro GD, Frijia F, Positano V, et al. Cardiac metabolism in a pig model of ischemia-reperfusion by cardiac magnetic resonance with hyperpolarized ¹³C-pyruvate. *IJC Metab Endocr*. 2015;6:17-23. <https://doi.org/10.1016/j.ijcme.2015.01.007>
- Yoshihara HAI, Bastiaansen JAM, Berthonneche C, Comment A, Schwitler J. An intact small animal model of myocardial ischemia-reperfusion: characterization of metabolic changes by hyperpolarized ¹³C MR spectroscopy. *Am J Physiol - Hear Circ Physiol*. 2015;309:H2058-H2066. <https://doi.org/10.1152/ajpheart.00376.2015>
- Reeder SB, Pineda AR, Wen Z, et al. Iterative decomposition of water and fat with echo asymmetry and least-squares estimation (IDEAL): application with fast spin-echo imaging. *Magn Reson Med*. 2005;54:636-644. <https://doi.org/10.1002/mrm.20624>
- Traectler J, Vishnevskiy V, Fuetterer M, Kozerke S. Joint image and field map estimation for multi-echo hyperpolarized ¹³C metabolic imaging of the heart. *Magn Reson Med*. 2021;86:258-276. <https://doi.org/10.1002/mrm.28710>
- Hill DK, Orton MR, Mariotti E, et al. Model free approach to kinetic analysis of real-time hyperpolarized ¹³C magnetic resonance spectroscopy

- data. *PLoS One*. 2013;8:e71996. <https://doi.org/10.1371/journal.pone.0071996>
25. Larson PEZ, Gordon JW. Hyperpolarized metabolic MRI—acquisition, reconstruction, and analysis methods. *Metabolites*. 2021;11(6):386. <https://doi.org/10.3390/metabo11060386>
26. Fernández-Jiménez R, Sánchez-González J, Agüero J, et al. Myocardial edema after ischemia/reperfusion is not stable and follows a bimodal pattern: imaging and histological tissue characterization. *J Am Coll Cardiol*. 2015;65:315–323. <https://doi.org/10.1016/j.jacc.2014.11.004>
27. Ibanez B, Aletas AH, Arai AE, et al. Cardiac MRI endpoints in myocardial infarction experimental and clinical trials: JACC scientific expert panel. *J Am Coll Cardiol*. 2019;74:238–256. <https://doi.org/10.1016/j.jacc.2019.05.024>
28. Tada Y, Yang PC. Myocardial edema on T2-weighted MRI: new marker of ischemia reperfusion injury and adverse myocardial remodeling. *Circ Res*. 2017;121:326–328. <https://doi.org/10.1161/CIRCRESAHA.117.311494>
29. Lopez D, Pan JA, Pollak PM, et al. Multi-parametric CMR imaging of infarct remodeling in a percutaneous reperfused Yucatan mini-pig model. *NMR Biomed*. 2017;30:1–11. <https://doi.org/10.1002/nbm.3693>
30. Garcia MJ, Kwong RY, Scherrer-Crosbie M, et al. State of the art: imaging for myocardial viability: a scientific statement from the American Heart Association. *Circ Cardiovasc Imaging*. 2020;13:1–18. <https://doi.org/10.1161/HCI.000000000000053>
31. Hansen ESS, Tougaard RS, Nørlinger TS, et al. Imaging porcine cardiac substrate selection modulations by glucose, insulin and potassium intervention: a hyperpolarized [^{13}C]pyruvate study. *NMR Biomed*. 2017;30:1–7. <https://doi.org/10.1002/nbm.3702>
32. Lau AZ, Miller JJ, Robson MD, Tyler DJ. Simultaneous assessment of cardiac metabolism and perfusion using copolarized [^{1-13}C]pyruvate and ^{13}C -urea. *Magn Reson Med*. 2017;77:151–158. <https://doi.org/10.1002/mrm.26106>
33. Fuetterer M, Busch J, Traechtler J, et al. Quantitative myocardial first-pass cardiovascular magnetic resonance perfusion imaging using hyperpolarized [^{1-13}C] pyruvate. *J Cardiovasc Magn Reson*. 2018;20:1–15. <https://doi.org/10.1186/s12968-018-0495-2>

KEY WORDS cardiac magnetic resonance relaxometry, chronic myocardial infarction, hibernating myocardium, hyperpolarized pyruvate, metabolic cardiac magnetic resonance imaging

APPENDIX For expanded Methods, Results, and Discussion sections as well as supplemental figures and tables, please see the online version of this paper.